

Reconciling simulated melting and ground-state properties of metals with a modified embedded-atom method potential

Gennady Sushko,¹ Alexey Verkhovtsev,^{1,2,*} Christian Kexel,^{1,3}
Andrei V. Korol,^{1,4} Stefan Schramm,^{2,3} and Andrey V. Solov'yov^{1,†}

¹*MBN Research Center, Altenhöferallee 3, 60438 Frankfurt am Main, Germany*

²*Frankfurt Institute for Advanced Studies, Ruth-Moufang-Str. 1, 60438 Frankfurt am Main, Germany*

³*Department of Physics, Goethe-Universität, Max-von-Laue-Str. 1, 60438 Frankfurt am Main, Germany*

⁴*Department of Physics, St. Petersburg State Maritime Technical University,
Leninskii prospekt 101, 198262 St. Petersburg, Russia*

We propose a modification of the embedded-atom method-type potential aiming at reconciling simulated melting and ground-state properties of metals by means of classical molecular dynamics. Considering titanium, magnesium, gold, and platinum as case studies, we demonstrate that simulations performed with the modified force field yield quantitatively correctly both the melting temperature of the metals and their ground-state properties. It is shown that the accounting for the long-range interatomic interactions noticeably affect the melting point assessment. The introduced modification weakens the interaction at interatomic distances exceeding the equilibrium one by a characteristic vibration amplitude defined by the Lindemann criterion, thus allowing for the correct simulation of melting, while keeping its behavior in the vicinity of the ground state minimum. The modification of the many-body potential has a general nature and can be applicable to metals with different characteristics of the electron structure as well as for many different molecular and solid state systems experiencing phase transitions.

I. INTRODUCTION

The melting of crystals and crystallization of liquids are of great scientific and technological significance. The solid-liquid phase boundary represents an important part of the phase diagram and is widely explored in material science, high-pressure physics, astrophysics, and geophysical sciences [1–3]. Along with experimental methods of studying phase transitions, classical molecular dynamics (MD) simulations [4, 5] represent a powerful tool which have an eminent research potential. It can provide insights into nanoscale structural features and thermo-mechanical properties of the system under study by means of advanced computer simulations [6]. Provided that interatomic potentials, which are used to model interactions in a system, correctly describe different system properties, classical MD simulations may become a low-cost alternative to experimental studies and allow one to reach the system sizes and time scales that are inaccessible by *ab initio* methods [7–10].

Despite the abundance of interatomic potentials for modeling metallic, organic, and biomolecular systems, and complex systems composed of such constituents [6, 11–13], the overwhelming majority of these functions are capable of reproducing only ground-state properties of a system. While matching the results of *ab initio* calculations of ground-state parameters, these force fields poorly describe highly-excited vibrational states when the system under study is far from the potential energy

minimum, that is the case when a phase transition occurs in the system [14, 15]. The proper quantitative description of phase transitions in general and the melting process in particular by means of MD simulations is a major scientific challenge that concerns metal materials [16, 17], as well as inorganic [18], and biomolecular systems, like proteins [19] or water [20, 21].

This paper aims at formulating a recipe for constructing an interatomic potential that is able to correctly reproduce both the melting temperature and the ground-state properties of metal systems by means of classical MD simulations. To achieve this goal, we propose a modification of the widely utilized embedded-atom method (EAM)-type potential [22, 23] and demonstrate its applicability to different metal systems. Our analysis has revealed that interatomic interactions at distances, exceeding the equilibrium distance by a characteristic vibration amplitude defined by the Lindemann melting criterion [14, 24], significantly affect the correctness of simulations. In order to reproduce accurately the value of the melting point, these interactions should be corrected as they are overestimated by conventional EAM-type potentials. The modified force field weakens the interatomic interactions at distances beyond the equilibrium point, thus yielding the correct value of melting temperature.

II. COMPUTATIONAL DETAILS

In the EAM approach, the total energy of a metal system is expressed via the energy F_i , obtained by embedding an atom i into the local electron density $\bar{\rho}_i$ provided by the remaining atoms of the system, and that of the short-range electrostatic interaction between atoms i and

* verkhovtsev@fias.uni-frankfurt.de

† On leave from A.F. Ioffe Physical-Technical Institute, Politekhnicheskaya ul. 26, 194021 St. Petersburg, Russia

j separated by a distance r_{ij} :

$$U(r_{ij}) = \sum_{i=1}^N \left[F_i(\bar{\rho}_i) + \frac{1}{2} \sum_{j \neq i} \phi(r_{ij}) \right]. \quad (1)$$

Different many-body potentials [25–28], that have such a general form, are capable of describing geometrical, mechanical, and energetic properties (e.g., cohesive energy, lattice parameters, and elastic constants), but can rarely reproduce the experimentally measured melting temperature. An illustrative case study is bulk titanium, whose melting temperature, as calculated using the many-body potentials which account for the interaction of a given atom with several surrounding atomic layers [29, 30], differ from experimental values by several hundred degrees [29, 31]. A similar order of discrepancy was observed also for other systems, such as gold and silicon, modeled using the original and more elaborated EAM potentials [32, 33]. Thus, it is essential to amend the existing force fields, so that they can reproduce correctly properties of both the ground- and finite-temperature states of metal systems.

In this work, we propose such a modification. The new potential $U_{\text{mod}}(r_{ij})$ should satisfy the principal condition that the curvature of the modified potential energy profile in the vicinity of the equilibrium point must coincide with that of the original potential. This condition is set to reproduce, with the new potential, ground-state properties which are governed by the behavior of the potential energy curve in the vicinity of the equilibrium point.

To properly simulate melting of metal systems, we introduce a modification that satisfies the above-defined condition. As an illustration, we add a linear function to the existing formula, so that the modified expression for the potential energy of the system reads as:

$$U_{\text{mod}}(r_{ij}) = U(r_{ij}) + B r_{ij} + C, \quad (2)$$

where $U(r_{ij})$ is the original EAM-type potential (1), and B and C are adjustable parameters. As shown below, the term $B r_{ij}$ makes the resulting potential steeper (less attractive) at interatomic distances exceeding the equilibrium point but, at the same time, it also slightly changes the depth of the potential well at the equilibrium point. The constant term C is thus introduced to discard the latter effect. As a case study, we used the exact form of the potential $U(r_{ij})$ which is based on the second-moment approximation of the tight-binding model [11]. According to this scheme [28, 34], the attractive many-body part of the potential is related to band energy and is expressed as a square-root of electron density, $F_i(\bar{\rho}_i) \sim \sqrt{\bar{\rho}_i}$. Both the attractive and repulsive terms are introduced in this approach in the exponential form [34, 35] which is commonly referred in the literature as to the Gupta potential [27]. The total potential energy of a system of N atoms

located at positions \mathbf{r}_i reads as:

$$U = \sum_{i=1}^N \left\{ \sum_{j \neq i} A \exp \left[-p \left(\frac{r_{ij}}{d} - 1 \right) \right] - \sqrt{\sum_{j \neq i} \xi^2 \exp \left[-2q \left(\frac{r_{ij}}{d} - 1 \right) \right]} \right\}. \quad (3)$$

Here, d is the first-neighbor distance, ξ is an effective overlap integral between electronic orbitals of neighboring atoms, q and p control the decay of the exponential functions and are related to bulk elastic constants [35]. We note that the introduced modification (2) is spiritually similar to the well-known Dzugutov pairwise potential [36] which was developed to model glass-forming liquid metals. The Dzugutov potential is constructed to suppress crystallization common to most monatomic systems by the introduction of a repulsive term representing the Coulomb interactions that are present in a liquid metal. The similar idea of increasing repulsion at large interatomic distances for modeling metals in highly-vibrational states far from the potential energy minimum is pursued with the introduced linear modification.

The impact of the modified potential was investigated by analyzing thermal, geometrical, and energetic properties of nanoscale samples composed of four representative metals, namely titanium, magnesium, gold, and platinum. A generality of the introduced correction is emphasized by considering metals with different characteristics of the electron structure, namely (i) s, p -bonding (Mg), (ii) transition metal with less than half-filled d band (Ti), (iii) transition metal with almost filled d band (Pt), and (iv) noble metal (Au).

We considered finite-size spherical nanoparticles with radii from 1 to 7 nm, cut from ideal hexagonal close-packed (hcp) (in the case of Ti and Mg) or face-centered cubic (fcc) (for Au and Pt) crystals. The nanoparticles were composed of approximately 300 to 80 000 atoms. The crystalline structures were constructed and optimized, and the MD simulations were carried out using the MBN Explorer software package [6]. Energy minimization was performed using the velocity-quenching algorithm. The MD simulations of the nanoparticle heating/melting were performed without boundary conditions in the NVT canonical ensemble. The temperature T was controlled by a Langevin thermostat with a damping coefficient of 1 ps^{-1} . The nanoparticles were heated up with a constant rate of 0.5 K/ps . The time integration of the equations of motion was done using the velocity-Verlet algorithm [37] with an integration time step of 5 fs. In all the calculations, the interatomic interactions were truncated at the cutoff radius r_c lying in the range between 6.6 and 7 Å, depending on the system. Parameter B was derived independently for each considered metal so that the extrapolated bulk melting point corresponds to the reference value. The parameter C was then tuned to reproduce the reference value of cohesive energy. Param-

TABLE I. Utilized parameters of the original (3) and the modified (2) EAM-type potentials describing the interactions in titanium, magnesium, gold, and platinum.

	d (Å)	A (eV)	p	ξ (eV)	q	Ref.	B (eV/Å)	C (eV)	r_c (Å)
Ti	2.95	0.153	9.25	1.88	2.51	[38]	0.0114	-0.060	7.0
Mg	3.21	0.029	12.82	0.50	2.26	[34]	0.0061	-0.032	7.0
Au	2.88	0.206	10.23	1.79	4.04	[34]	0.0065	-0.034	6.65
Pt	2.78	0.297	10.61	2.70	4.00	[34]	0.0064	-0.031	6.6

eters of the potential (3) and the correction (2) utilized in this work are summarized in Table I.

In the proposed modification, the linear term $Br_{ij} + C$ is responsible for a monotonic increase of the potential at large distances. In this case the cutoff distance is set to the value at which the modified potential (2) is equal to zero. The parametrization of the original EAM-type potential for titanium, given in Table I, was obtained in Ref. [38] with the cutoff distance of 4.2 Å as another adjustable parameter. The other three metals are described in this work with the parametrization by Cleri and Rosato [34] where the summation in the EAM-type potential was "... extended up to the fifth neighbors for cubic structures". The analysis of radial distribution function for gold and platinum demonstrates that the fifth neighbors in these metals are located at the distance 6.45 and 6.15 Å from the given atom, respectively. These values are slightly smaller than the cutoff values which we have used in the simulations, see Table I. In reference [34], hcp metals were described "... with cutoff values ranging between $\sqrt{11/3}d$ and $\sqrt{5}d$ " where d is the first-neighbor distance. The original cutoff for titanium, as formulated in Ref. [34], thus lies in the range from 5.65 to 6.60 Å which is smaller than the cutoff used in our simulations. Similarly, the original cutoff for magnesium lies in the range between 6.15 and 7.2 Å and corresponds to the value of $r_c = 7$ Å which we have adopted in the simulations.

In theory, a cutoff distance should be set on the grounds that forces at larger interatomic distances are negligibly small, so that distant interactions are infinitesimally weak and could be excluded from consideration. However, there is no unique way to define the cutoff distance in a general case; thus, the value utilized in every simulation defines its accuracy and corresponding computational costs. We found that the ground-state properties like lattice constants are nicely described even with small values of cutoff (e.g., $r_c = 4.2$ Å for titanium [38]), while the estimated value of melting temperature turned out to be cutoff-dependent. Our analysis has demonstrated that an explicit account of very distant interatomic interactions when using the original EAM-type potential (3) does not allow for a proper quantitative description of melting, and the potential modification is required to bring the calculated melting temperature closer to the experimental values. In the performed simulations, the cutoff distance is set to the value at which the modified potential is equal to zero, thereby significantly reducing cutoff effects in the modified potential compared

TABLE II. Comparison of ground-state parameters of the modeled crystals for different specifications of the potential.

	U_{orig}	U_{mod}	exp.	U_{orig}	U_{mod}	exp.
	Ti			Mg		
a , Å	2.92	2.92	2.95	3.20	3.20	3.21
c , Å	4.76	4.76	4.68	5.22	5.22	5.21
E_{coh} , eV	5.04	4.85	4.87	1.52	1.49	1.52
	Au			Pt		
a , Å	4.07	4.05	4.08	3.93	3.91	3.92
E_{coh} , eV	3.78	3.80	3.78	5.85	5.84	5.85

to the original approach.

III. RESULTS AND DISCUSSION

To quantify the effect due to the potential modification, we have analyzed first the ground-state geometrical and energetic properties of the samples, namely lattice parameters and cohesive energy (see table II). The quantity E_{coh} represents the cohesive energy per atom of an infinitely large ideal crystal, which was obtained by extrapolating the binding energies of Ti_N , Mg_N , Au_N and Pt_N ($N \approx 300 - 80\,000$) nanoparticles to the $N \rightarrow \infty$ limit. Table II demonstrates that, similar to the case of the original potential (the column labeled as " U_{orig} "), the modification of the potential (the column " U_{mod} ") allows one to reproduce experimental values [39] with a relative discrepancy of less than 2%.

As another benchmark of the modified potential, we have also analyzed vacancy formation energy. This quantity is given by

$$E_{\text{vf}} = E_{N-1} - \frac{N-1}{N} E_N. \quad (4)$$

where E_N and E_{N-1} are the energies of a perfect crystal and a vacancy-formed structure after relaxation, and N is the number of atoms in the simulation box. To calculate E_{vf} , the following procedure was adopted. A perfect crystal was created, which spans at least three cutoff distances in each direction. The crystal comprising N atoms was relaxed using periodic boundary conditions. Then, one atom was removed from the crystal. The crystal now comprising $N-1$ atoms was relaxed again using periodic boundary conditions. To check the consistency of the results, we have analyzed the samples of different size, containing from about 500 up to 2048 atoms.

Table III presents the vacancy formation energy calculated with the original (the column " U_{orig} ") and the modified (the column " U_{mod} ") potentials. The calculated values are compared with available experimental data and the results of earlier DFT and classical calculations. This analysis demonstrates that the numbers obtained with the original EAM-type potential (3) and its modification (2) are consistent with one another and agree in general with the existing experimental and theoretical values.

Melting temperature of the finite-size nanoparticles was estimated from analyzing the temperature dependence of the heat capacity, $C_V = (\partial E / \partial T)_V$, defined as a derivative of the internal energy of the system with respect to temperature. A sharp maximum of C_V was attributed to the nanoparticle melting. The bulk melting temperature was estimated by extrapolating the obtained values to the $N \rightarrow \infty$ limit according to the Pawlow law [10, 51, 52]. It describes the dependence of the melting temperature of spherical particles on the number of atoms they are composed of as $T_m = T_m^{\text{bulk}} - \alpha N^{-1/3}$, where T_m^{bulk} is the melting temperature of a bulk material and α is the factor of proportionality. Thus evaluated values of melting temperature are summarized in Figure 1 and Table IV for all the studied metals.

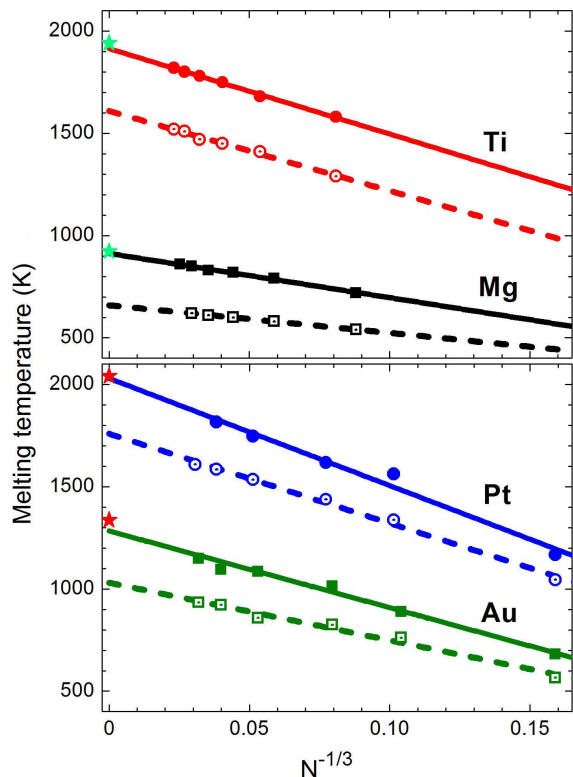


FIG. 1. Melting temperature of spherical Ti_N , Mg_N , Au_N , and Pt_N nanoparticles calculated by means of the original, U (open symbols), and modified, U_{mod} (closed symbols), potential. Lines represent the linear extrapolation of the calculated numbers to the bulk ($N \rightarrow \infty$) limit. Experimental values of melting temperature are shown by stars.

In Figure 1, symbols illustrate the results of the simulations for the finite-size nanoparticles. The estimated values of the bulk melting temperature obtained with the use of the original potential (3) (open symbols) lead to a significant deviation of about 300 K from the experimental values which are marked by stars. The situation changes drastically when introducing the linear correction to the original potential. Figure 1 illustrates that the use of the modified force field (closed symbols) leads to a much better correspondence of the bulk-limit extrapolations with the experimental values for all studied metals. The extrapolation procedure yields the values of the melting temperature presented in Table IV are in good agreement with the reference values with the relative discrepancy of a few (1 – 4%) percent.

In order to shed light on the physical effects which are behind the above-described improvement, we have analyzed melting of the studied metal systems in terms of the Lindemann criterion [14]. It states that melting occurs because of vibrational instability, i.e. a crystalline structure melts when the average amplitude of thermal vibrations of atoms is relatively high compared to interatomic distances. This condition can be expressed as $\langle (\delta u)^2 \rangle^{1/2} > \delta_L d$, where δu is the atomic displacement, δ_L is the Lindemann parameter typically equal to 0.10 – 0.15, and d is the interatomic distance [15].

Our analysis has revealed that interatomic interactions at distances, exceeding the equilibrium distance by a characteristic vibration amplitude defined by the Lindemann criterion, significantly affect the correctness of simulations. To elaborate on this issue, the following procedure has been adopted. We have analyzed the potential energy surfaces (PES) for the studied metal systems. As a case study, we considered large 6 nm-radius nanoparticles with the optimized structure; positions of all atoms in the system except for a given one were fixed. The movable atom was displaced from its equilibrium position and the interaction energy was calculated. Then, the energy of the perturbed system was subtracted from the energy of the fully optimized system. The resulting PES for the metal nanoparticles are presented in Figure 2. Each panel shows several isolines corresponding to a given energy difference between the optimized and the perturbed systems. For the sake of clarity, this quantity has been converted into temperature.

The figure illustrates that the modified potential (solid curves), due to the additional linear term, makes the resulting potential steeper at large interatomic distances, as compared to the original EAM-type potential (dashed curves). For instance, in the case of titanium (left panel), the displacement of an atom for about 0.3 Å, that is approximately 1/10 of the closest interatomic distance ($d_{\text{Ti}} = 2.95$ Å), results in the energy difference of about 0.17 eV that corresponds to 2000 K. Thus, interatomic interactions at distances, exceeding the equilibrium distance by a characteristic vibration amplitude δu , are overestimated by conventional EAM-type potentials and should be corrected in order to reproduce the quantita-

TABLE III. Vacancy formation energy (in eV) calculated with the original (U_{orig}) and the modified (U_{mod}) potential. The calculated values are compared with available experimental data and the results of earlier calculations. The experimental methods comprise positron annihilation (PA), thermal expansion (TE) and quenching (Q) measurements. Earlier theoretical calculations performed by means of density functional theory are labeled as DFT, and LDA/GGA denote the local density or generalized gradient approximations. EAM denotes the classical MD simulations performed using an EAM-type potential.

	this work		exp. data	calculations
	U_{orig}	U_{mod}		
Ti	1.56	1.52	1.55 [40]	1.56 (EAM) [38]
			1.27 ± 0.05 (PA) [41]	2.14 (DFT-LDA) [42]
				1.97 (DFT-GGA) [43]
Mg	0.60	0.62	0.58 ± 0.01 (TE) [44]	0.88 (EAM) [45]
			0.79 ± 0.03 (Q) [46]	0.77 – 0.80 (DFT-GGA) [47]
Au	0.61	0.64	$0.62 - 0.67$ (TE) [48]	0.60 (EAM) [28]
			$0.70 - 1.10$ (Q) [48]	0.75 (EAM) [34]
Pt	1.16	1.14	1.35 ± 0.09 (PA) [49]	1.28 (EAM) [28]
				1.15 (DFT-LDA) [50]
				1.18 (DFT-GGA) [50]

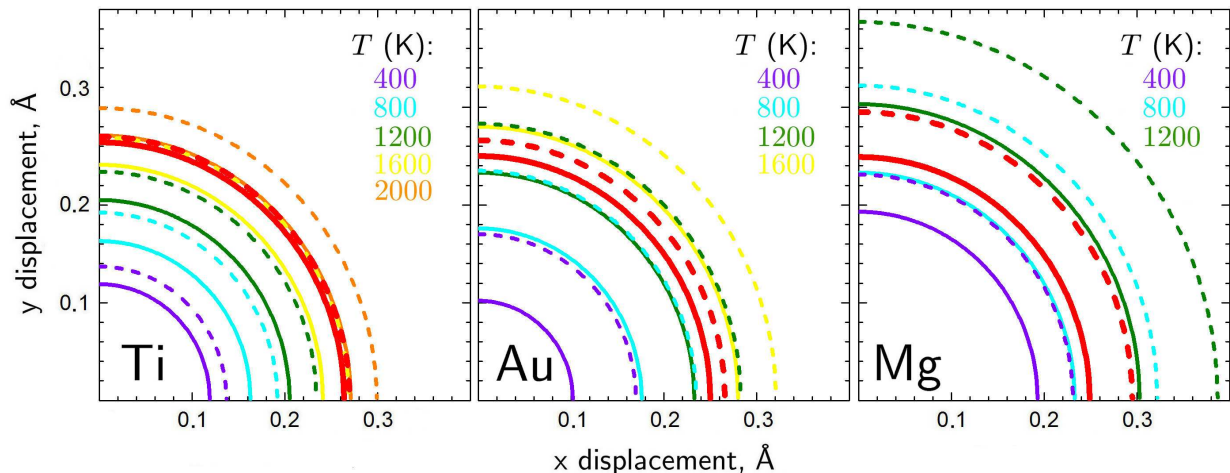


FIG. 2. Potential energy surface for 6 nm-radius metal nanoparticles whose constituent atoms interact via the original (dashed lines) or the modified (solid lines) potentials. The thick dashed and solid (red) lines denote the energy difference corresponding to the predicted bulk melting temperatures (see Table IV).

TABLE IV. Melting temperature T_m^{bulk} (in kelvin) of different metals which is evaluated on the basis of the performed MD simulations.

	U	U_{mod}	exp.
Mg	658	913	923
Au	1030	1284	1337
Ti	1610	1915	1941
Pt	1759	2030	2041

tively correct value of the melting point. A more accurate description of the interatomic interaction in the region beyond the equilibrium distance allows one to handle the problem of the accurate description of thermal properties of metal materials.

IV. CONCLUSION

In summary, we have formulated a recipe for modifying the embedded-atom method-type potential that reconciles the simulated melting temperature and ground-state properties of metals by means of molecular dynamics simulations. It has been demonstrated that the modified many-body potential reduces the gap between the simulated and the experimental values of bulk melting temperature of metal systems, such as titanium, magnesium, gold and platinum, down to about a few percent and also does not affect the accuracy of description of ground-state properties like the lattice parameters, cohesive energy and the energy of vacancy formation. The physical background behind this improvement is that the modified potential weakens the interatomic interactions at large distances, which are typically overestimated by

the conventional embedded-atom method. A proper account for the long-distance interatomic interactions has been found to be crucial for a quantitatively accurate simulation of melting and other excited vibrational state properties of the system being far from the potential energy minimum. The introduced modification of the embedded-atom method-type potential can be utilized for an accurate modeling of other metals and alloys that have been treated with the use of this approach so far.

ACKNOWLEDGEMENTS

The work was supported by the European Commission (the FP7 Multi-ITN Project "ARGENT", grant agreement no. 608163). The possibility to perform computer simulations at the Frankfurt Center for Scientific Computing using the LOEWE-CSC cluster is gratefully acknowledged. AVK acknowledges the support from the Alexander von Humboldt Foundation.

-
- [1] Bang J H and Suslick K S 2010 *Adv. Mater.* **22** 1039
 - [2] Yoo C S, Holmes N C, Ross M, Webb D J and Pike C 1993 *Phys. Rev. Lett.* **70** 3931
 - [3] Belonoshko A B *et al* 2008 *Phys. Rev. Lett.* **100** 135701
 - [4] Rapaport D C 2004 *The Art of Molecular Dynamics Simulation* (Cambridge: Cambridge University Press)
 - [5] Leach A 2001 *Molecular Modelling: Principles and Applications* (Harlow, England: Prentice Hall)
 - [6] Solov'yov I A, Yakubovich A V, Nikolaev P V, Volkovets I and Solov'yov A V 2012 *J. Comput. Chem.* **33** 2412
 - [7] Zhao G *et al* 2013 *Nature* **497** 643
 - [8] Vashishta P, Kalia R K and Nakano A 2006 *J. Phys. Chem. B* **110** 3727
 - [9] Verkhovtsev A V, Yakubovich A V, Sushko G B, Hanauske M and Solov'yov A V 2013 *Comput. Mater. Sci.* **76** 20
 - [10] Yakubovich A V, Sushko G, Schramm S and Solov'yov A V 2013 *Phys. Rev. B* **88** 035438
 - [11] Rafii-Tabar H and Mansoori G A 2010 *Encyclopedia of Nanoscience and Nanotechnology* vol 4 ed H S Nalwa (Valencia, CA: American Scientific Publishers) p 231
 - [12] MacKerell Jr A D *et al* 1998 *The Encyclopedia of Computational Chemistry* vol 1 ed P von Rague Schleyer (Chichester: John Wiley & Sons, Inc.) p 271
 - [13] Monticelli L and Tieleman D P 2004 *Biomolecular Simulations: Methods and Protocols* ed L Monticelli and E Salonen (New York: Springer Science+Business Media) p 197
 - [14] Lindemann F A 1910 *Z. Physik* **11** 609
 - [15] Rice S A 2008 *Advances in Chemical Physics* vol 137 (Hoboken, NJ: John Wiley & Sons)
 - [16] Los J H and Pellenq R J M 2010 *Phys. Rev. B* **81** 064112
 - [17] Kexel Ch, Schramm S and Solov'yov A V 2015 *Eur. Phys. J. B* **88** 221
 - [18] Hussien A, Yakubovich A V, Solov'yov A V and Greiner W 2010 *Eur. Phys. J. D* **57** 207
 - [19] Freddolino P L, Harrison C B, Liu Y and Schulten K 2010 *Nat. Phys.* **6** 751
 - [20] Vega C and Abascal J L F 2011 *Phys. Chem. Chem. Phys.* **13** 19663
 - [21] Shvab I and Sadus R J 2012 *Phys. Rev. E* **85** 051509
 - [22] Daw M S and Baskes M I 1984 *Phys. Rev. B* **29** 6443
 - [23] Daw M S, Foiles S M and Baskes M I 1993 *Mater. Sci. Rep.* **9** 251
 - [24] Nelson D R 2002 *Defects and Geometry in Condensed Matter Physics* (Cambridge: Cambridge University Press)
 - [25] Finnis M W and Sinclair J E 1984 *Philos. Mag. A* **50** 45
 - [26] Sutton A P and Chen J 1990 *Philos. Mag. Lett.* **61** 139
 - [27] Gupta R P 1981 *Phys. Rev. B* **23** 6265
 - [28] Rosato V, Guillope M and Legrand B 1989 *Philos. Mag. A* **59** 321
 - [29] Kim Y-M, Lee B-J and Baskes M I 2006 *Phys. Rev. B* **74** 014101
 - [30] Baskes M I and Johnson R A 1994 *Modelling Simul. Mater. Sci. Eng.* **2** 147
 - [31] Sushko G B, Verkhovtsev A V, Yakubovich A V, Schramm S and Solov'yov A V 2014 *J. Phys. Chem. A* **118** 6685
 - [32] Lewis L J, Jensen P and Barrat J-L 1997 *Phys. Rev. B* **56** 2248
 - [33] Ryu S, Weinberger C R, Baskes M I and Cai W 2009 *Modelling Simul. Mater. Sci. Eng.* **17** 075008
 - [34] Cleri F and Rosato V 1993 *Phys. Rev. B* **48** 22
 - [35] Tomanek D, Aligia A A and Balseiro C A 1985 *Phys. Rev. B* **32** 5051
 - [36] Dzugutov M 1992 *Phys. Rev. A* **46** 2984
 - [37] Frenkel D and Smit B 2001 *Understanding Molecular Simulation: From Algorithms to Applications* (San Diego, CA: Academic Press)
 - [38] Lai W S and Liu B X 2000 *J. Phys.: Condens. Matter* **12** L53
 - [39] Kittel C 1995 *Introduction to Solid State Physics* (New York: John Wiley & Sons, Inc.)
 - [40] Shestopal V O 1966 *Fiz. Tverd. Tela* **7** 3461 (Engl. Transl. *Sov. Phys. Solid State* **7** 2798)
 - [41] Hashimoto E, Smirnov E A and Kino T, 1984 *J. Phys. F: Met. Phys.* **14** L215
 - [42] Le Bacq O, Willaime F and Pasturel A 1999 *Phys. Rev. B* **59** 8508
 - [43] Raji A T, Scandolo S, Mazzarello R, Nsengiyumva S, Härting M and Britton D T 2009 *Philos. Mag.* **89** 1629
 - [44] Janot C, Malléjac D and George B 1970 *Phys. Rev. B* **2** 3088
 - [45] Johansen C G, Huang H and Lu T-M 2009 *Comput. Mater. Sci.* **47** 121
 - [46] Tzanetakis P, Hillairet J and Revel G 1976 *Phys. Status Solidi B* **75** 433
 - [47] Jund Ph, Viennois R, Colinet C, Hug G, Fèvre M and Tédénac J-C 2013 *J. Phys.: Condens. Matter* **25** 035403
 - [48] Jongenburger P 1957 *Phys. Rev.* **106** 66 (and references therein)
 - [49] Schaefer H-E 1987 *Phys. Status Solidi A* **102** 47
 - [50] Mattsson T R and Mattsson A E 2002 *Phys. Rev. B* **66** 214110
 - [51] Pawlow P 1909 *Z. Phys. Chem.* **65** 1
 - [52] Qi Y, Çağın T, Johnson W L and Goddard III W A 2001 *J. Chem. Phys.* **115** 385